

Designing LF Talkback for a Magnetic Base Station

Author: Ruan Lourens
Microchip Technology Inc.

INTRODUCTION

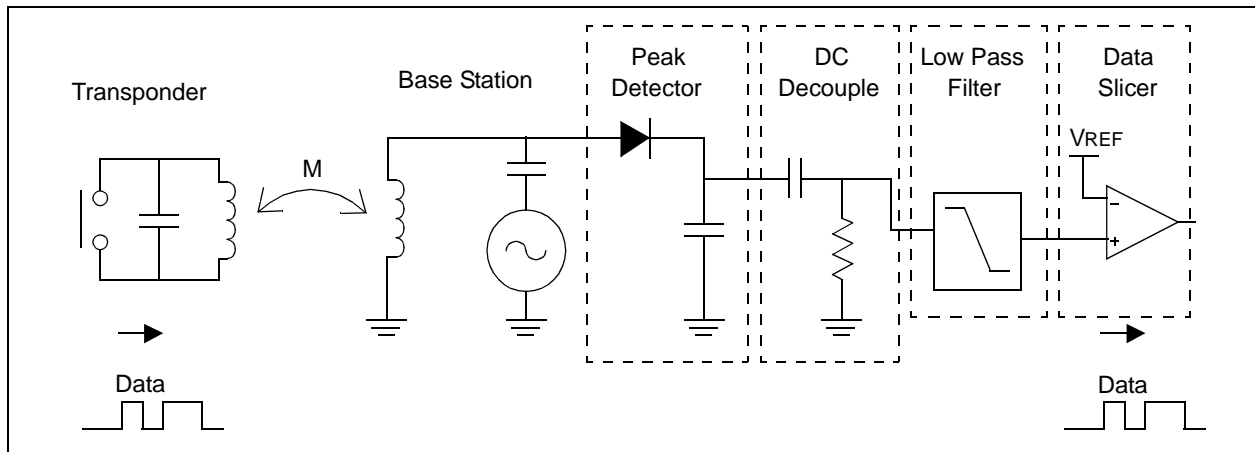
This application note builds on application note AN232 *Low Frequency Magnetic Transmitter Design* (DS00232). It covers the design process to implement LF Talkback functionality. AN232 covers some of the magnetism basics and design principles to implement the drive circuitry. LF Talkback generally refers to the process in which a transponder can communicate back to a magnetic transmitter base station by loading the generated magnetic field. By measuring the small changes in the transmitter coil's voltage, used to generate the field, the communications' data is extracted. LF Talkback is commonly used in RFID, automotive transponders, active transponders, and many other bidirectional LF communications topologies.

This document will cover the different stages needed to implement a typical LF Talkback system and explain the process in choosing the different stage characteristics. It explains the various performance and cost trade-offs made for the reference design and how it can be adapted to better suit the readers needs.

MAIN BUILDING BLOCKS

Figure 1 shows the main building blocks that make up the LF Talkback system described in this document. The base station generates a strong magnetic field by setting up resonance in a serial resonant tank. The circulating energy in the resonant tank typically generates 300V peak-to-peak voltage across the transmitting antenna coil at 125 kHz. The transponder, whether active or passive, is magnetically coupled to the base station's transmitting coil and the transponder's magnetic loading has a small effect on the quality factor (Q) of the transmitter resonant tank. Talkback is accomplished by changing or modulating the magnetic loading and can be observed as small voltage changes across the base station's resonant transmitter coil. The difficulty is to detect a few mV of modulation on the 300V peak-to-peak carrier.

FIGURE 1:



AN912

A high voltage peak detector is used to extract the basic envelope of the base station's resonant tank. The output of the peak detector will be 150 VDC with about 2V peak-to-peak of carrier ripple at 125 kHz and then about 2 mV of modulated signal. The modulation signal strength is mostly dependent on the distance between the transponder and the transmitter coil as the magnetic coupling decreases to the third power of the distance between the two devices. The next stage is a passive high-pass filter to decouple or block the high DC voltage. The DC extracted voltage is then fed into a low-pass filter, leaving the required modulating signal. The last stage is the data slicer that compares the modulating signal to some reference to extract the original signal sent by the transponder.

LF Talkback receiver can be thought of as detecting and decoding an amplitude modulation (AM) signal that has a very low modulation index on a relatively large carrier.

SYSTEM ASSUMPTIONS

The LF Talkback system designed in this document is targeted for a LF base station that has the following characteristics and is based on the design as per AN232:

- The LF Talkback signal is amplitude modulated at 200 μ s multiples. This is also referred to as the basic pulse element period or TE.
- The tank is driven by a 12V half-bridge driver.
- The tank inductance is 162 μ H and the resonant capacitor is 10 nF with a resonant frequency of 125 kHz.
- The tank Q is 25. As a result, the tank or carrier voltage is 300V peak-to-peak or 150V 0-to-peak.
- Transponder induced modulation of 2 mV in magnitude needs to be detected.

To get an understanding of the impedances involved, lets consider the following: using Equation 1, the equivalent parallel resistance of the tank is 3.18 k Ω . The additional parallel impedance that a transponder represents to induce a 2 mV signal on the tank is in the order of 500 M Ω . What the LF Talkback system detects is the result of a 500 M Ω resistor being switched in and out in parallel with the tank at the data rate. Therefore, it is very important that the peak detector have a high-impedance at the data rate to maintain good sensitivity.

EQUATION 1: THE EFFECTIVE PARALLEL IMPEDANCE OF A RESONANT TANK

$$R_{PARALLEL} = 2\pi L F C Q$$

L = Tank inductance in H = 162 μ H

Fc = Center frequency of tank = 125 kHz

Q = Tank quality factor = 25

THE PEAK DETECTOR

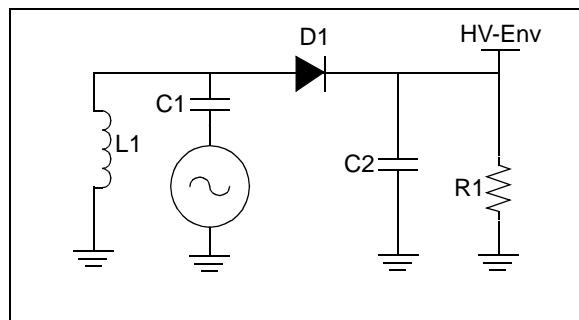
There are a number of aspects to consider in designing a peak detector for this application:

1. The peak detector has to be able to operate at the high voltages of the resonant tank.
2. Maintain a good tank Q or, in other words, it should not add unnecessary loading on the main resonant tank. If it does load the tank, it will result in a lower modulation voltage induced by the transponder.
3. Reduce carrier ripple as far as possible.
4. Maintain the modulation signal.
5. Have a fast large swing dynamic response and be able to settle quickly after the field is turned on.
6. Cost of the system.

Some of the peak detector requirements are conflicting and as a result, the designer has to find an acceptable compromise with the final system performance in mind. One can sacrifice a specific parameter and make up for it in a later stage where optimization of that aspect is easily accomplished.

As an example to optimize requirement 3, one needs to increase the size of the capacitor C2 (Figure 2), but that will negatively affect requirements 2, 4 and 5 if a passive peak detector is used. An active peak detector could have solved the conflict, but at the 600V swing, one has little choice but to use a passive peak detector while maintaining a low-cost design. A relatively low capacitance value is chosen for C1 of 1 nF. This maintains the dynamic response requirement for settling quickly after the field is applied and does not load the tank unnecessarily. Capacitor C2 should have at least a 300 VDC peak rating and a high tolerance capacity is acceptable to save cost. An ultra fast diode is required in the peak detector with a 400V or better rating and low junction capacitance. A UF1005 diode was chosen, it has a 600V rating and 10 pF of junction capacitance.

FIGURE 2:



The envelope detector with only D1 and C2 has a greatly different response to increasing and decreasing voltage amplitudes of the resonant tank. The voltage designated by the signal HV_Env (Figure 2) rises quickly with increasing tank amplitudes because D1 has a low-impedance in forward conduction. The tank voltage decreases slower when the tank amplitude is lowered because C2 can only discharge through D1, which has a high-impedance in the reverse direction. The situation can be remedied to some extent by the introduction of R1 which helps to discharge C2, but the value of R1 should be high enough to maintain a good tank Q as per requirement 2 above. A 10 M Ω value for R1 works well, but note that R1 needs to be implemented as a series of two resistors. This is done to stay within the safe voltage range of 0805 resistors are used.

The 125 kHz carrier ripple voltage, without R1, is about 2V peak-to-peak and is due to the junction capacitance and reverse leakage of D1. The addition of R1 has little effect on the ripple voltage, but does improve the detectors dynamic performance at the data rate. The carrier ripple voltage will be filtered out at a later stage where a more effective solution can be implemented.

THE DC DECOUPLER CONFLICTS

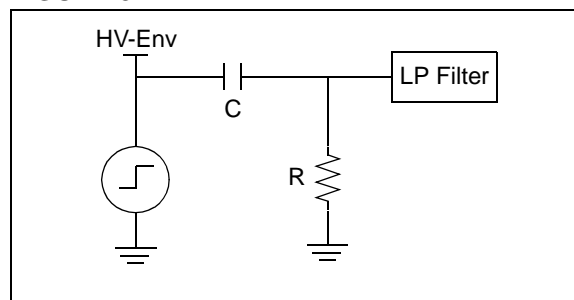
The HV_Env signal (Figure 2) consists of three main components:

1. A 150V DC signal, as a result of the peak detector.
2. 2V peak-to-peak ripple voltage at the carrier frequency.
3. The modulated data signal at a TE of 200 μ s and a 2 mV peak-to-peak amplitude, highest fundamental harmonic content is at 2.5 kHz [$1/(2*200 \mu$ S)], irrespective of the modulation scheme used (i.e., Manchester, PWM etc.).

The aim of the decoupling stage is to reject the high DC voltage without adding unnecessary loading to the tank via the peak detector. It should also have a fast dynamic response and stabilize quickly after the tank is energized. The dynamic response of the LF Talkback system is the major design hurdle to overcome as far as the decoupling stage is concerned. The problem is aggravated when the transponder needs to communicate on the LF link soon after the base station communicated with the transponder.

The base station typically uses On Off Keying (OOK) modulation to communicate to the transponder. This means the tank resonance is completely halted and then started up to transfer data via the magnetic link. The decoupling stage experiences large “step” responses as data is transmitted to the transponder. The tank can ramp up to its full resonant amplitude in 100 μ s to 400 μ s depending on the drive system used.

FIGURE 3:



The system can be simplified as shown in Figure 3. The output of the peak detector can be simplified as the step response source with a 150V amplitude that also has the carrier and data signals superimposed on it as described earlier. The output response of the decoupling stage is given by Equation 2. This is also the input signal to the low-pass filter.

EQUATION 2:

$$V = 150e^{-t/\tau}$$

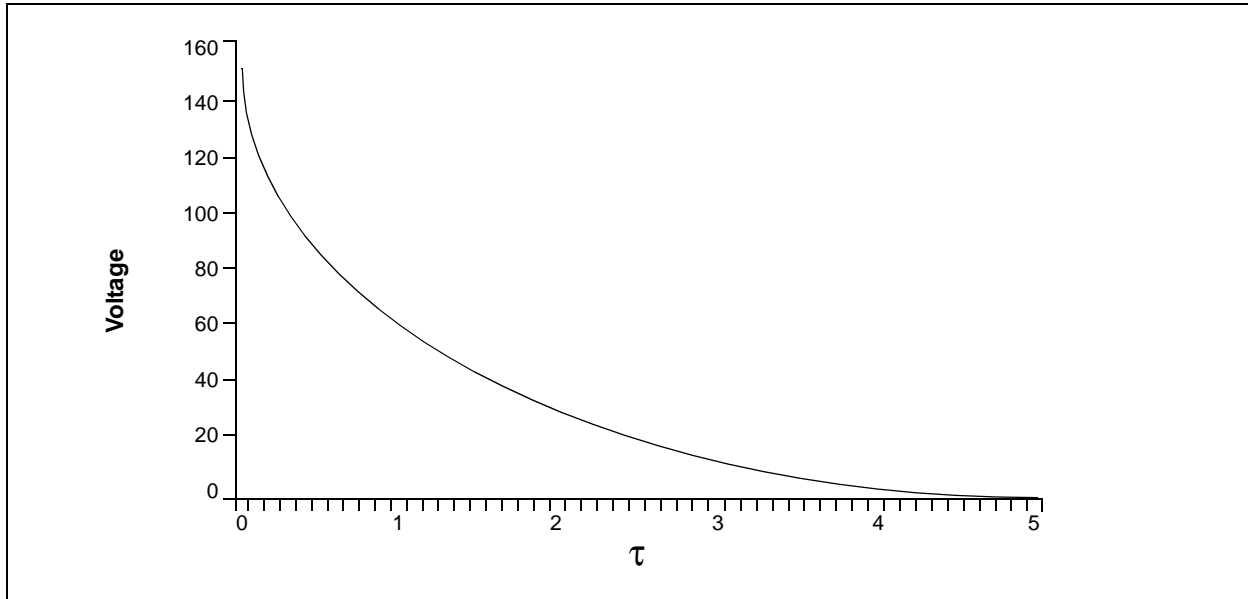
$$\tau = RC$$

It is useful to think in terms of τ (RC time constant) because the voltage across the resistor reduces by a factor of 0.368 as every τ second elapses. The exponential decay curve, for the voltage across R, is shown in Figure 4 and indicates that the initial voltage decays rapidly, but settles out slower as the voltage is reduced across the resistor. The system must be allowed to settle for a long enough period so that the step response voltage has reduced to a voltage that is smaller than the modulation voltage.

The required value for RC, or τ , can be calculated using Equation 3, based on the following assumptions:

- The system needs to be able to start LF communications 200 μ s after the resonant tank has stabilized.
- The decoupler should settle to at least half the data modulation voltage.

FIGURE 4:



EQUATION 3:

$$\tau = \frac{t_{SETTLE}}{\ln(V_o/V_{SETTLE})}$$

$t_{SETTLE} = 200 \mu s$
 $V_o = 150 V$
 $V_{SETTLE} = 1 mV$

Using Equation 3, τ was calculated to be 16.78 μs . The question now is how will the data signal be affected by the decoupling stage? The decoupling stage, shown in Figure 3, is also a high-pass filter and it was calculated that the RC time constant needs to be 16.78 μs to satisfy the transient response requirement. The 3 dB cutoff frequency, for a τ , of 16.78 μs is calculated as 9.48 kHz using Equation 4. This means that the decoupling stage will only pass one quarter of the original data signal at 2.5 kHz, which is not desirable from a signal-to-noise ratio perspective.

EQUATION 4:

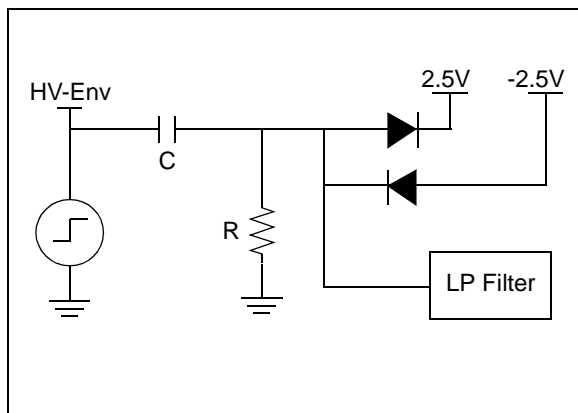
$$F_c = \frac{1}{2\pi\tau}$$

From a data signal conservation, or high-pass filter point-of-view, τ should be at least 64 μs . The conflicting τ requirement shows that a basic high-pass filter is not sufficient as a decoupler unless either dynamic response or data signal strength is sacrificed.

AN IMPROVED DECOUPLER

From the previous section, it is clear that a high-pass filter is needed with either a controllable τ or a nonlinear τ that is based on the voltage across the output of the decoupler. Both approaches will be covered and the latter solution is shown in Figure 5.

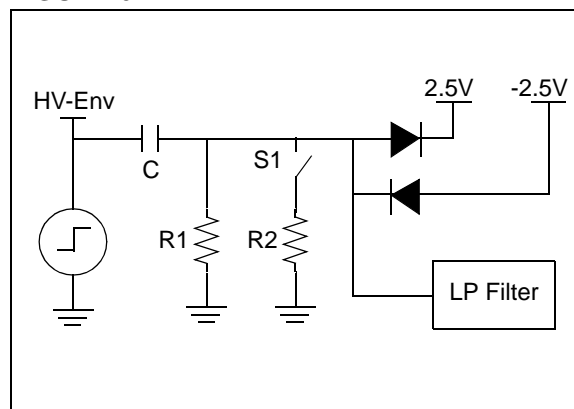
FIGURE 5:



The addition of the two diodes, shown in Figure 5, results in a nonlinear τ with respect to voltage because it effectively lowers the R component of τ whenever the voltage is either above 3.1V or below -3.1V. In a practical circuit, the diodes will start conducting when the tank is turned on and the voltage, across the resistor R, is around 3 volts, after the tank has stabilized. Previously, τ was calculated with an initial voltage of 150 VDC, but if the calculation is repeated with an initial voltage of 3 VDC, then the required τ comes to 25 μ s. The RC time constant is improved by a significant factor from 16.78 μ s to 25 μ s with the additional diodes, however, it is still not in the 64 μ s ball park. The diodes have the additional advantage in that they protect the low-pass filter from the large positive and negative voltages that develop across the resistor during tank transient periods.

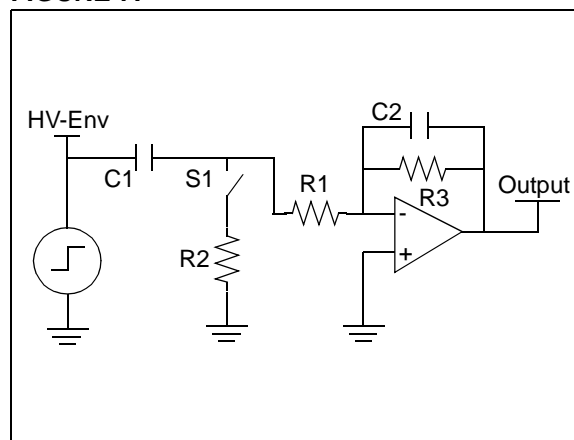
The final part to solving the time constant problem is to add an additional resistor via a switch, as shown in Figure 6. The switch is closed to reduce τ from 64 μ s to 25 μ s during transient periods and opened while data is received via the LF Talkback link.

FIGURE 6:



The final part of the decoupling stage is to lower the output impedance by adding an active buffer in the form of an inverting amplifier that has an input resistance equal to R1. The use of an inverting amplifier has the additional advantages that it can add gain and a single order low-pass filter to the decoupler, as shown in Figure 7. The gain is equal to the ratio of R3/R1, and the low pass cutoff frequency is set by R3 and C2, as per Equation 4. The low pass cutoff frequency should be chosen at least two decades above the main low-pass filter, otherwise it will have an undesirable effect on the envelope response. For single ended 5V designs, the gain should be limited to about 10 dB to avoid amplifier saturation due to carrier ripple and data modulation.

FIGURE 7:



THE LOW PASS FILTER STAGE

The output signal from the decoupling stage consists of the 125 kHz carrier ripple and the modulated data signal, if one ignores the dynamic response signal. The carrier ripple is about 300 mV peak-to-peak. The data is 4 mV peak-to-peak with 6 dB of gain of the decoupler and a cutoff frequency at about 10 kHz. The aim of the low-pass filter stage is to amplify the data signal at 2.5 kHz and to filter out the carrier ripple in the most effective manner.

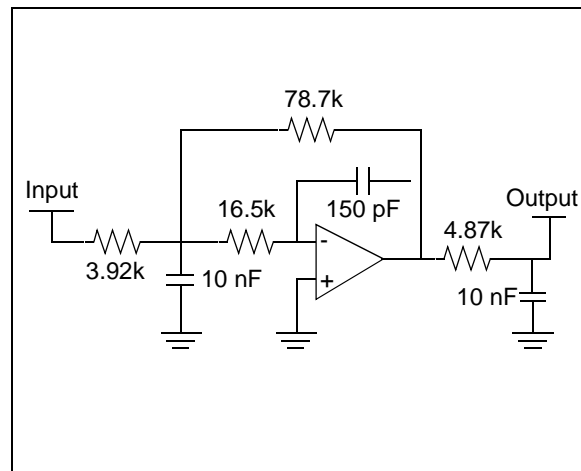
The three most common active filter topologies used are the Chebyshev, Butterworth and Bessel filters. The Chebyshev filter has the steepest transition from pass band to stop band, but has ripple in the pass band. The Butterworth filters have the flattest pass band response, but does not have such a steep transition as the Chebyshev. The Bessel filter has a linear phase response with a smooth transition from pass to stop band. It seems the Chebyshev filter would best be suited for this application, but the frequency response does not tell the whole story.

The data signal is amplitude modulated and the tank has steep transient response dynamics. As a result, the filter should have a stable and flat transient response. The Chebyshev filter has a very sharp frequency cutoff response, but has the worst transient response of the three filter topologies. The Chebyshev filter also has an underdamped step response with overshoot and ringing. The Butterworth filter has a better transient response, but still some overshoot. The Bessel filter has the worst response from a frequency perspective, but has the best transient response as a result of its linear phase characteristics. There are of course other active filter topologies such as elliptical, state variable, biquad and more, but a Bessel filter has adequate performance for the application.

The data signal, in this example, has maximum modulation frequency of 2.5 kHz or a T_E of 200 μ s. A Bessel filter, with a cutoff frequency of $1/(2.2T_E) = 2.27$ kHz, would be ideal from a noise rejection point of view, but a 2.5 kHz cutoff was chosen to minimize symbol overlap. The target is to design a filter with sufficient performance using a single operational amplifier in order to reduce the system cost. A dual operational amplifier can then be used because the decoupling stage also uses an amplifier. A third order Bessel filter can now be implemented with the remaining amplifier.

The filter gain is the final aspect to specifying the Bessel filter. Using Microchip's FilterLab[®] program, one can get the response for a unity gain – 2.5 kHz, 3d order Bessel filter. At 125 kHz, the filter has 93 dB of attenuation and the input ripple amplitude is 300 mV peak-to-peak. Assuming the filter should have an output ripple of no more than 1 mV peak-to-peak with 12 dB of headroom for noise, coupled through the supply line, then one needs at least 62 dB of attenuation. This leaves 31 dB of allowable gain from the third order filter. For the design, a gain of 20 or 26 dB was chosen, leaving some additional headroom for ripple rejection. The 3d order low-pass Bessel filter is shown in Figure 8 and has a $F_c = 2.5$ kHz and 26 dB of gain. Please note that the circuit shown in Figure 8 has a fairly high output impedance at the data rate, but the output of the filter will be driving a high-impedance load, and this is therefore acceptable.

FIGURE 8:



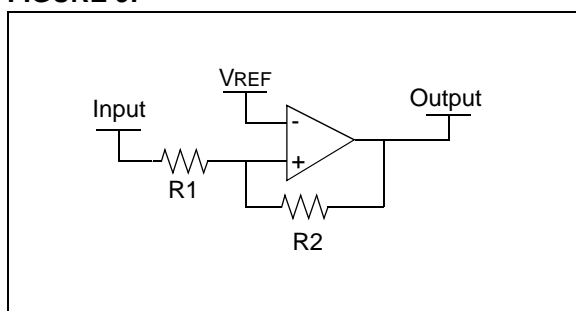
DATA SLICER

The data slicer is essentially a comparator with some input hysteresis voltage to reduce the influence of noise. The overall system gain of the decoupler and the low-pass filter, at 2.5 kHz, is about 29 dB or a factor of 28, and the system should be able to detect the 2 mV data signal. The headroom between the hysteresis and data signal was chosen to be about 9 dB or a factor of 2.8. This means that the minimum input voltage to overcome the data slicer hysteresis is about 700 μ V. This translates to 20 mV of hysteresis for the data slicer. Most comparators have some deliberate hysteresis to improve noise stability and this amount should be extracted from the required hysteresis when calculating the amount of required feedback. Figure 9 shows a typical hysteresis circuit and Equation 5 can be used to calculate the amount of hysteresis for a single-ended circuit.

EQUATION 5:

$$V_{HYST} = \frac{R1}{R2} V_{DD}$$

FIGURE 9:



For example, if a comparator with 10 mV of offset and hysteresis is used, then an additional 10 mV of hysteresis should be added. The resistor R2 is calculated to be 5 M Ω for a V_{DD} of 5 VDC and R1 = 10 k Ω .

AN EXAMPLE SYSTEM

A complete circuit with layout, based on the foregoing design study, is shown in this section. The circuit diagram is shown in Figure 11. The top and bottom layout for the printed circuit board is shown in Figure 12. The PIC16F648A was chosen for the application, it has two comparators, a USART, EEPROM and 4k of Flash program memory. The PIC16F648A can be substituted with its smaller program memory equivalents, the PIC16F627A or PIC16F628A. The filter examples have been converted to operate from a single 5 VDC supply. The 2.5 VDC virtual ground is provided by the voltage divider consisting of R23 and R24, shown in Figure 11. The Reference voltage does not have to be actively buffered, it is lightly loaded. A 0.1 μ F decoupling capacitor C10 is sufficient for noise reduction.

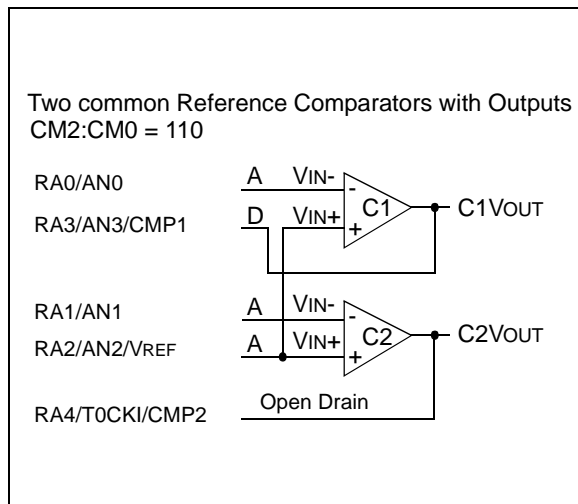
A TC4422 FET driver, U1, drives the resonant tank consisting of L1 and C2. The tank generates a strong magnetic field and the voltage at the test pin TP1 can reach 320V peak-to-peak. The main antenna, L1, is an air-cored inductor with a 25 mm radius and 41 turns of 26-gage wire, and has a 162 μ H inductance. The inductor L2 and capacitors C3 and C4 are not populated and are added to the printed circuit board to test alternative antennas. The peak detector consists of D1, C5, R1, and R2, and is connected to the decoupling stage via C6. The RC time constant of the decoupling tank is set by C6 and R4 to 177 μ s, which is substantially longer than the minimum filter requirement of 64 μ s. Resistor R3 is used to change the decoupler's time constant to 11 μ s by changing RB7 from a high-impedance input to an output.

The decoupler buffer, U2:A, has a gain of 6 dB and a low pass cutoff frequency at 9.8 kHz, set by R5 and C8. The R22 resistor is used to ensure the proper DC bias of the stage, but does not have a significant effect on the overall sensitivity. The output of the decoupler is connected to the input of the low pass Bessel filter and one of the PIC16F648's comparators. The remaining op amp, U2:B, is used for the Bessel filter. U2 is a dual MCP6002 op amp that has a GBWP of 1 MHz. The filter components should have better tolerances than the high voltage components and 1% resistors. The 5% NP0 capacitors are recommended.

AN912

The PIC16F648A has various comparator options. Figure 10 shows the topology that was chosen for this application. The main filter output signal “ENV_IN” is connected to comparator C1 via RA0. Resistor R10 was placed in series with the output of the filter to have 10 k Ω impedance. Together with the 4.99 M Ω resistor, R11 adds an additional 10 mV of hysteresis. The comparator has a combined offset and hysteresis of 10 mV, in the worst case, making for a total of 20 mV of hysteresis, in the worst case, and about 15 mV on average. It should be noted that the output of comparator C1 has to be inverted by setting bit C1INV, in the CMCON register. The output inversion is needed to result in positive feedback, via R11, as is shown in Figure 9. At first glance, it seems as if R10 can be removed and R11 changed to a 2.43 M Ω resistor, but the capacitor C12 will cause delay and that can lead to instability.

FIGURE 10:



There are additional aspects around the decoupler that need to be explained for the system as it is implemented. The port pin RB7 is essentially an open circuit when it is configured as an input and the input voltage is between VDD (5V) and ground. All the general purpose I/O pins have internal ESD protection diodes that become conductive when a pin voltage is forced outside the VDD to ground range. This has the effect that the RC time constant for the decoupling stage is reduced to 11 μ s from 177 μ s whenever the “BIAS” signal is about 0.6V above VDD, or below ground even if RB7 is configured as an input. The addition of R3 works well, but keep in mind, the stable DC voltage for signal “A”, shown in Figure 11, is 2.5 VDC and the signal “BIAS” is either 5V or ground. One can implement one of two approaches to correctly bias the signal at point “A”.

The first solution is to toggle RB7 between high and low with a 50% duty cycle at 20 kHz or more. This is equivalent to connecting the “BIAS” signal to the desired 2.5 VDC. This is only done for a short period after the tank is turned on or off, to force the decoupler to stabilize faster than it would with just R4. The second approach is to force the signal “A” in the required direction. The voltage at “A” will go above VDD if the tank is turned on after it has been turned off for some time. The “BIAS” signal can be grounded during the turn-on transient period until the voltage at point “A” reaches the desired 2.5 VDC or VREF. By monitoring either of the comparator output signals, it is possible to detect when the voltage at point A goes through VREF. Pin RB7 can be turned into an input as soon as the cross over is detected resulting in a decoupler RC time constant of 177 μ s. The filters introduce delay that cause some overshoot of the voltage at point “A”. The overshoot can be resolved by allowing some additional stabilizing time with R4, before LF communication is interpreted as data.

SYSTEM MODIFICATIONS

The system can be modified to better suit the user's requirements. The first aspect is to change the Bessel filter for a different LF Talkback TE. The rule of thumb is to set the filter's 3 dB cutoff frequency to $F_c = 1/(2 \cdot TE)$. The new values for the Bessel filter, with a 400 μ s TE, is given in Table 1.

TABLE 1:

R6 = 3.57k	R7 = 15.0k	R8 = 71.5k	R9 = 4.42k
R10 = 5.62k	C9 = C12 = 22 nF	C11 = 330 pF	

In addition to changing the filter cutoff frequency for a TE of 400 μ s, it is possible to increase the gain up to 18 dB and still maintain the carrier rejection chosen. It is also possible to increase C6 to a 4.7 nF capacitor, but please note that this will increase the transient response period. Increasing C6 will not have a dramatic influence on the overall system performance and it is not recommended.

LONGER TRANSIENT STABILIZING PERIOD

The example system was designed with the requirement that LF Talkback communications should be able to start 200 μ s after the resonant tank has stabilized. The tank itself takes 100 μ s to 400 μ s to stabilize sufficiently, depending on the drive mechanism. The example circuit should be able to start LF Talkback communications with 2 mV of data modulation after 350 μ s to 450 μ s, from when the tank is turned. The exact period depends on the residual charge in the peak detector from previous transmissions.

The system can be simplified and improved if the system allows for a longer transient stabilizing period before LF Talkback communications are initiated. The peak detector capacitor, C5, can be increased proportionally to the longer stabilizing period, but not by more than a factor of about 3, otherwise it can influence data modulation sensitivity. R1 and R2 tank resistors should be reduced if C5 is increased, but not proportionally, it will effect sensitivity. The combined value for R1 and R2 should be no less than 4 M Ω .

Capacitor C6 can also be increased, but it will not have a dramatic performance increase. The biggest advantage of a longer transient stabilizing period is that bias resistor R3 can be increased. Increasing the value of R3 will result in a slower change in the signal at point "A", which means the tank can be controlled more accurately during the transient period.

INCREASED DATA SENSITIVITY

Increasing the system's sensitivity to the modulated data signal can increase the LF Talkback range. A solution has been partly described in the previous section; increase TE from 200 μ s to 400 μ s and then increase the gain by up to 18 dB. The component values for a system with a 400 μ s TE, or a center frequency of 1.25 kHz, and a gain of 100, or a 14 dB increase, is described in Table 2 below. This approach decreases the dynamic range that may or may not be used depending on how well the transponder loads the resonant tank.

TABLE 2:

R6 = 2.26k	R7 = 10.5k	R8 = 226k	R9 = 4.42k
R10 = 5.62k	C9 = 33 nF	C11 = 100 pF	C12 = 22 nF

Another solution is to remove resistor R11 to get the maximum sensitivity from the comparator, but this will also increase noise in the data. Another quick solution is to increase the gain of the decoupler buffer by up to 10 dB and lower the decoupler cutoff frequency by about half the gain increase ratio.

The existing design makes use of a 3d order Bessel filter. For improved noise reduction, increase the order of the filter and add more gain per stage. This would typically be done if a TE of 200 μ s or 100 μ s, is desired with more sensitivity than can be reliably obtained with the example system.

DRIVE SYSTEM

The example circuit uses a half-bridge driver based on the TC range of FET drivers from Microchip. To increase the transient response period of the tank, start the tank in Full-bridge mode until the desired tank amplitude is reached and the tank oscillation is maintained in Half-bridge mode. This method is described in AN232 *Low Frequency Magnetic Transmitter Design*.

CONCLUSION

This LF Talkback Design application note can be used to implement a cost-effective system to be used in RFID, passive keyless entry and other bidirectional transponder based technologies. The example circuit can be used as a basis for further hardware and firmware development to suit the user's requirements.

APPENDIX A: SCHEMATICS

FIGURE 11: LF BASE STATION

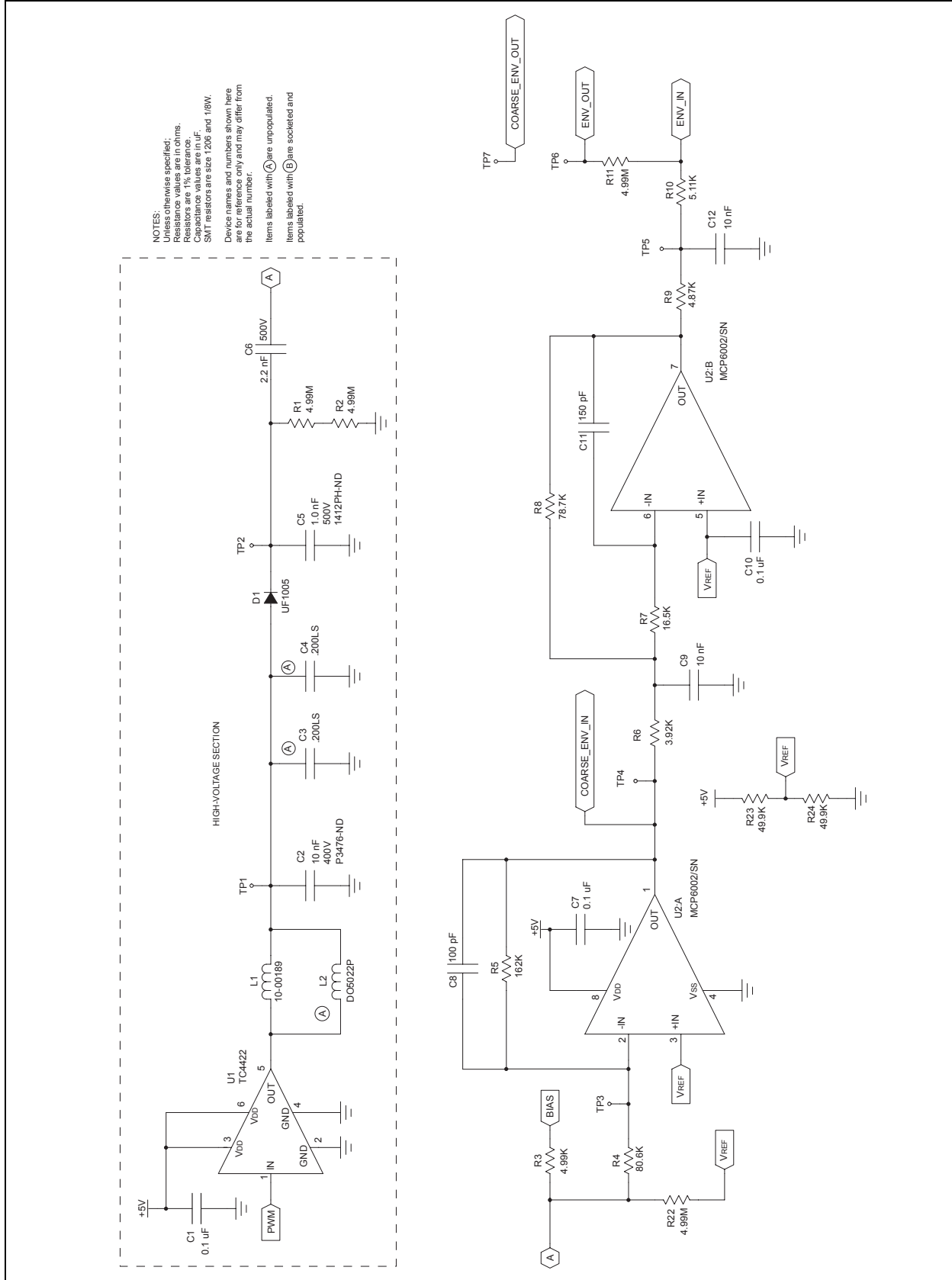
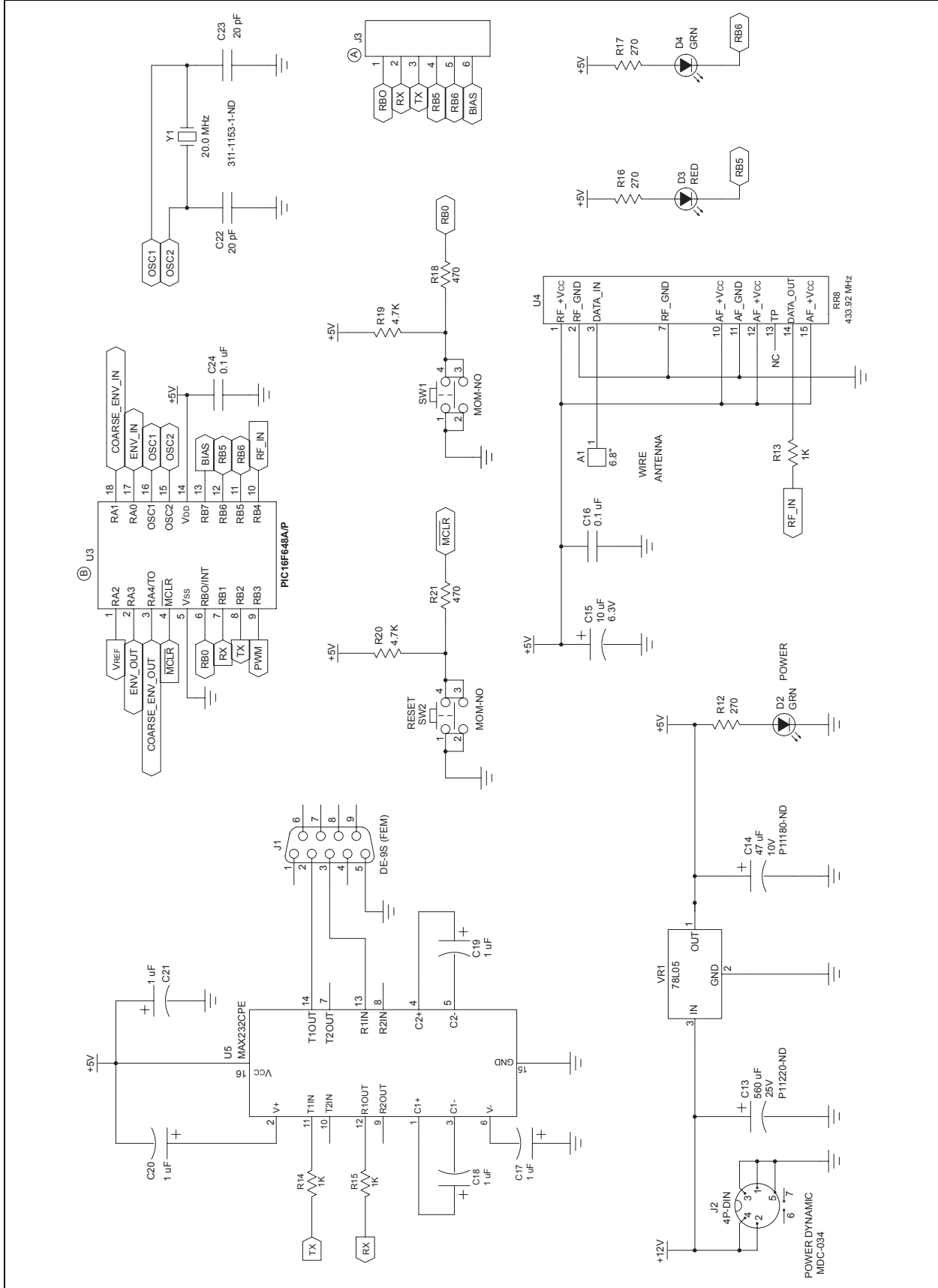


FIGURE 12: LF BASE STATION (Continued)



AN912

FIGURE 13: BOTTOM SIDE

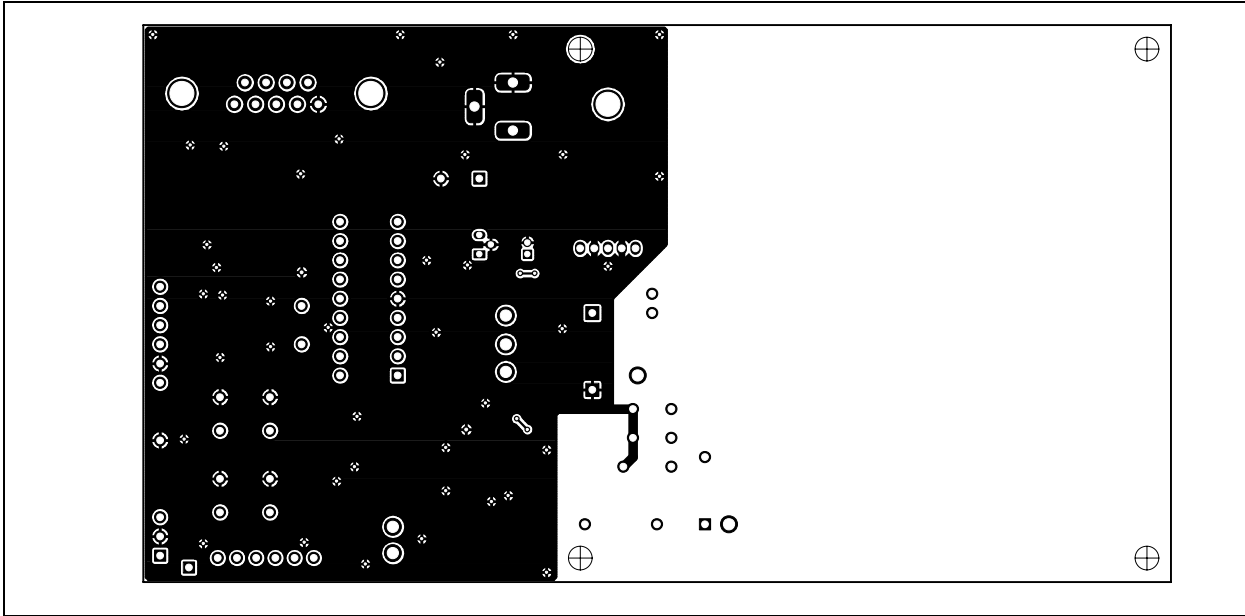


FIGURE 14: TOP SIDE

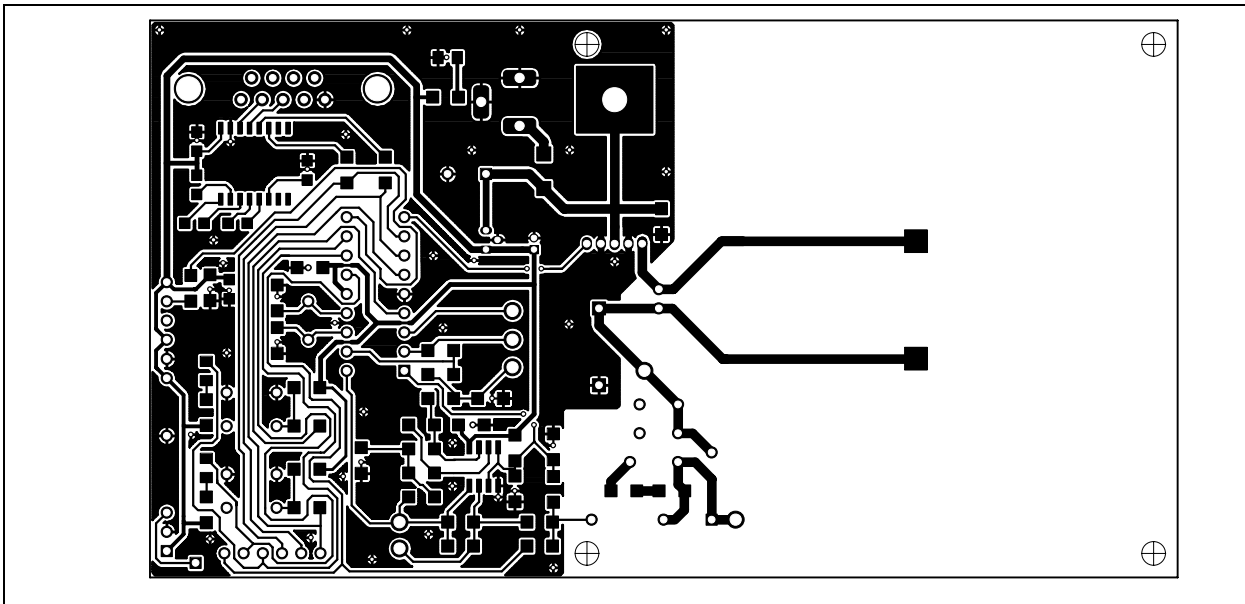
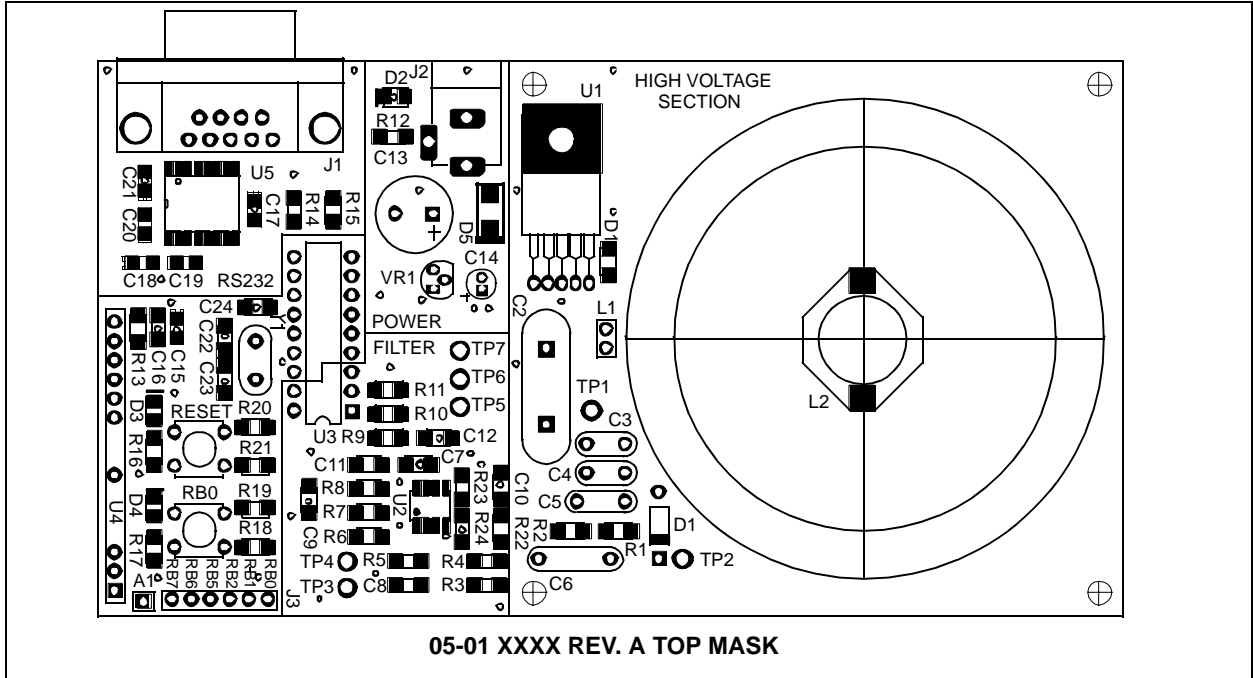


FIGURE 15: TOP MASK



AN912

NOTES:

Note the following details of the code protection feature on Microchip devices:

- Microchip products meet the specification contained in their particular Microchip Data Sheet.
- Microchip believes that its family of products is one of the most secure families of its kind on the market today, when used in the intended manner and under normal conditions.
- There are dishonest and possibly illegal methods used to breach the code protection feature. All of these methods, to our knowledge, require using the Microchip products in a manner outside the operating specifications contained in Microchip's Data Sheets. Most likely, the person doing so is engaged in theft of intellectual property.
- Microchip is willing to work with the customer who is concerned about the integrity of their code.
- Neither Microchip nor any other semiconductor manufacturer can guarantee the security of their code. Code protection does not mean that we are guaranteeing the product as "unbreakable."

Code protection is constantly evolving. We at Microchip are committed to continuously improving the code protection features of our products. Attempts to break Microchip's code protection feature may be a violation of the Digital Millennium Copyright Act. If such acts allow unauthorized access to your software or other copyrighted work, you may have a right to sue for relief under that Act.

Information contained in this publication regarding device applications and the like is intended through suggestion only and may be superseded by updates. It is your responsibility to ensure that your application meets with your specifications. No representation or warranty is given and no liability is assumed by Microchip Technology Incorporated with respect to the accuracy or use of such information, or infringement of patents or other intellectual property rights arising from such use or otherwise. Use of Microchip's products as critical components in life support systems is not authorized except with express written approval by Microchip. No licenses are conveyed, implicitly or otherwise, under any intellectual property rights.

Trademarks

The Microchip name and logo, the Microchip logo, Accuron, dsPIC, KEELOQ, MPLAB, PIC, PICmicro, PICSTART, PRO MATE and PowerSmart are registered trademarks of Microchip Technology Incorporated in the U.S.A. and other countries.


AmpLab, FilterLab, microID, MXDEV, MXLAB, PICMASTER, SEEVAL, SmartShunt and The Embedded Control Solutions Company are registered trademarks of Microchip Technology Incorporated in the U.S.A.

Application Maestro, dsPICDEM, dsPICDEM.net, dsPICworks, ECAN, ECONOMONITOR, FanSense, FlexROM, fuzzyLAB, In-Circuit Serial Programming, ICSP, ICEPIC, microPort, Migratable Memory, MPASM, MPLIB, MPLINK, MPSIM, PICKit, PICDEM, PICDEM.net, PICTail, PowerCal, PowerInfo, PowerMate, PowerTool, rfLAB, rfPIC, Select Mode, SmartSensor, SmartTel and Total Endurance are trademarks of Microchip Technology Incorporated in the U.S.A. and other countries.

Serialized Quick Turn Programming (SQTP) is a service mark of Microchip Technology Incorporated in the U.S.A.

All other trademarks mentioned herein are property of their respective companies.

© 2004, Microchip Technology Incorporated, Printed in the U.S.A., All Rights Reserved.

 Printed on recycled paper.

**QUALITY MANAGEMENT SYSTEM
CERTIFIED BY DNV
== ISO/TS 16949:2002 ==**

Microchip received ISO/TS-16949:2002 quality system certification for its worldwide headquarters, design and wafer fabrication facilities in Chandler and Tempe, Arizona and Mountain View, California in October 2003. The Company's quality system processes and procedures are for its PICmicro® 8-bit MCUs, KEELOQ® code hopping devices, Serial EEPROMs, microperipherals, nonvolatile memory and analog products. In addition, Microchip's quality system for the design and manufacture of development systems is ISO 9001:2000 certified.



WORLDWIDE SALES AND SERVICE

AMERICAS

Corporate Office

2355 West Chandler Blvd.
Chandler, AZ 85224-6199
Tel: 480-792-7200
Fax: 480-792-7277
Technical Support: 480-792-7627
Web Address: <http://www.microchip.com>

Atlanta

3780 Mansell Road, Suite 130
Alpharetta, GA 30022
Tel: 770-640-0034
Fax: 770-640-0307

Boston

2 Lan Drive, Suite 120
Westford, MA 01886
Tel: 978-692-3848
Fax: 978-692-3821

Chicago

333 Pierce Road, Suite 180
Itasca, IL 60143
Tel: 630-285-0071
Fax: 630-285-0075

Dallas

4570 Westgrove Drive, Suite 160
Addison, TX 75001
Tel: 972-818-7423
Fax: 972-818-2924

Detroit

Tri-Atria Office Building
32255 Northwestern Highway, Suite 190
Farmington Hills, MI 48334
Tel: 248-538-2250
Fax: 248-538-2260

Kokomo

2767 S. Albright Road
Kokomo, IN 46902
Tel: 765-864-8360
Fax: 765-864-8387

Los Angeles

18201 Von Karman, Suite 1090
Irvine, CA 92612
Tel: 949-263-1888
Fax: 949-263-1338

San Jose

1300 Terra Bella Avenue
Mountain View, CA 94043
Tel: 650-215-1444
Fax: 650-961-0286

Toronto

6285 Northam Drive, Suite 108
Mississauga, Ontario L4V 1X5, Canada
Tel: 905-673-0699
Fax: 905-673-6509

ASIA/PACIFIC

Australia

Suite 22, 41 Rawson Street
Epping 2121, NSW
Australia
Tel: 61-2-9868-6733
Fax: 61-2-9868-6755

China - Beijing

Unit 706B
Wan Tai Bei Hai Bldg.
No. 6 Chaoyangmen Bei Str.
Beijing, 100027, China
Tel: 86-10-85282100
Fax: 86-10-85282104

China - Chengdu

Rm. 2401-2402, 24th Floor,
Ming Xing Financial Tower
No. 88 TIDU Street
Chengdu 610016, China
Tel: 86-28-86766200
Fax: 86-28-86766599

China - Fuzhou

Unit 28F, World Trade Plaza
No. 71 Wusi Road
Fuzhou 350001, China
Tel: 86-591-7503506
Fax: 86-591-7503521

China - Hong Kong SAR

Unit 901-6, Tower 2, Metroplaza
223 Hing Fong Road
Kwai Fong, N.T., Hong Kong
Tel: 852-2401-1200
Fax: 852-2401-3431

China - Shanghai

Room 701, Bldg. B
Far East International Plaza
No. 317 Xian Xia Road
Shanghai, 200051
Tel: 86-21-6275-5700
Fax: 86-21-6275-5060

China - Shenzhen

Rm. 1812, 18/F, Building A, United Plaza
No. 5022 Binhe Road, Futian District
Shenzhen 518033, China
Tel: 86-755-82901380
Fax: 86-755-8295-1393

China - Shunde

Room 401, Hongjian Building, No. 2
Fengxiangnan Road, Ronggui Town, Shunde
District, Foshan City, Guangdong 528303, China
Tel: 86-757-28395507 Fax: 86-757-28395571

China - Qingdao

Rm. B505A, Fullhope Plaza,
No. 12 Hong Kong Central Rd.
Qingdao 266071, China
Tel: 86-532-5027355 Fax: 86-532-5027205

India

Divyasree Chambers
1 Floor, Wing A (A3/A4)
No. 11, O'Shaughnessy Road
Bangalore, 560 025, India
Tel: 91-80-2290061 Fax: 91-80-2290062

Japan

Benex S-1 6F
3-18-20, Shinyokohama
Kohoku-Ku, Yokohama-shi
Kanagawa, 222-0033, Japan
Tel: 81-45-471- 6166 Fax: 81-45-471-6122

Korea

168-1, Youngbo Bldg. 3 Floor
Samsung-Dong, Kangnam-Ku
Seoul, Korea 135-882
Tel: 82-2-554-7200 Fax: 82-2-558-5932 or
82-2-558-5934

Singapore

200 Middle Road
#07-02 Prime Centre
Singapore, 188980
Tel: 65-6334-8870 Fax: 65-6334-8850

Taiwan

Kaohsiung Branch
30F - 1 No. 8
Min Chuan 2nd Road
Kaohsiung 806, Taiwan
Tel: 886-7-536-4818
Fax: 886-7-536-4803

Taiwan

Taiwan Branch
11F-3, No. 207
Tung Hua North Road
Taipei, 105, Taiwan
Tel: 886-2-2717-7175 Fax: 886-2-2545-0139

EUROPE

Austria

Durisolstrasse 2
A-4600 Wels
Austria
Tel: 43-7242-2244-399
Fax: 43-7242-2244-393

Denmark

Regus Business Centre
Lautrup høj 1-3
Ballerup DK-2750 Denmark
Tel: 45-4420-9895 Fax: 45-4420-9910

France

Parc d'Activite du Moulin de Massy
43 Rue du Saule Trapu
Batiment A - Ier Etage
91300 Massy, France
Tel: 33-1-69-53-63-20
Fax: 33-1-69-30-90-79

Germany

Steinheilstrasse 10
D-85737 Ismaning, Germany
Tel: 49-89-627-144-0
Fax: 49-89-627-144-44

Italy

Via Quasimodo, 12
20025 Legnano (MI)
Milan, Italy
Tel: 39-0331-742611
Fax: 39-0331-466781

Netherlands

P. A. De Biesbosch 14
NL-5152 SC Drunen, Netherlands
Tel: 31-416-690399
Fax: 31-416-690340

United Kingdom

505 Eskdale Road
Winnersh Triangle
Wokingham
Berkshire, England RG41 5TU
Tel: 44-118-921-5869
Fax: 44-118-921-5820

01/26/04